Analytical model of chromatic dispersion effect in an analog fiber link with RF up-conversion

Antonio Alves Ferreira Júnior, Olympio Lucchini Coutinho, Carla de Sousa Martins, José Antônio Justino Ribeiro, Vilson Rosa de Almeida & José Edimar Barbosa Oliveira

***Abstract*—This paper addresses the subject of optical fiber chromatic dispersion effect on the performance of an analog optical link. An intermediate frequency signal directs modulate a laser diode and by using a dual-drive electrooptic Mach-Zehnder modulator a radio-frequency up-conversion is achieved. A direct-detection link model which emphasizes both the modulator electronic drive and the dispersion characteristic of a linear optical fiber is discussed. With Mach-Zehnder modulator biased at the nonlinear points, the effect of chromatic dispersion on the detected electrical power may be mitigated with the optical bandwidth increasing. An exact frequency domain analytical model which yields a rather insightful analysis of the link performance is discussed. The model usefulness is illustrated by predicting the dependence of the performance of a direct-detection optical fiber link with respect to the link length. Numerical preliminary results for a link which comprises optoelectronic components and has potential for practical applications are given.**

***Index Terms*—Analog optical fiber link, chromatic dispersion, dual-drive Mach-Zehnder modulator, RF up-conversion.**

I. Introduction

Due to the evidence that the microwave photonic technology will be playing a major role in global interconnectivity, many efforts have been direct toward researches and development on the field of optical fiber link. The microwave photonics technology focuses on generation, processing, control and transmission of radio-frequency (RF) signals by using photonic devices. A great deal of emphasis continues to be driven by military and commercial demands, which aim at performance on the subjects of photonic generation and processing of RF signals, microwave photonic filters, antenna-remoting and -beamforming, radio-over-fiber (RoF), and so on [1]-[8].

As an illustrations, a central office which is connected to a large number of base stations through optical fiber can be used in a high capacity metropolitan optical fiber network to distributed signals from various communications systems to the users, or to other optical fiber network area, as illustrated in Fig. 1(a) [9]-[10]. Aiming at aerospace and electronic warfare applications, the remote radar antenna could be placed at a distance of several kilometers from the central office and the generated radar signals could be distributed to other antennas to tracking an aircraft, or to other central offices [11]-[14]. This versatility is interesting because the human resources and the equipments can be allocated in a safety and controlled place, while the remote radar antenna is located at field, as suggested in Fig. 1(b).

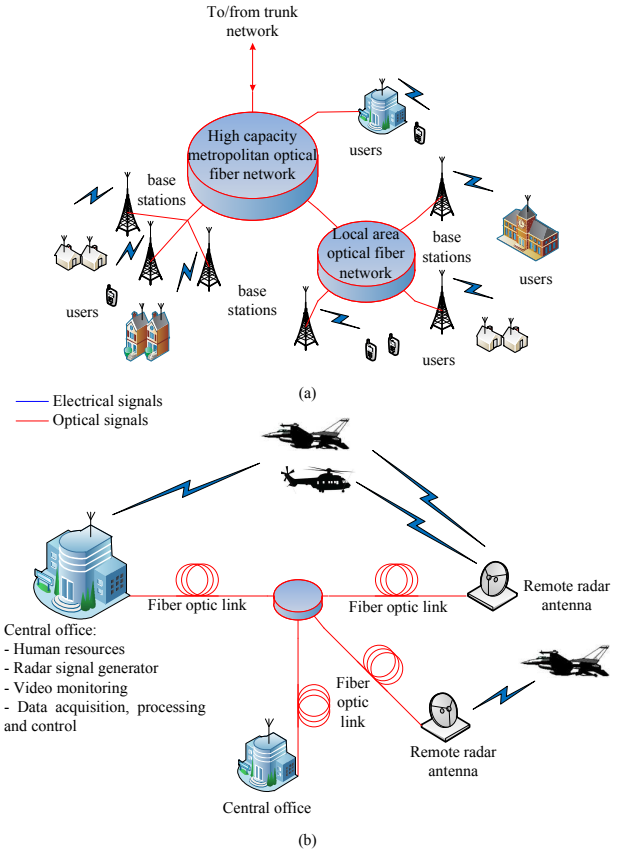

Fig. 1. Fiber optic links (a) for data system communications, and (b) aiming at aerospace and electronic warfare applications.

Manuscript received August 2013. Current version published October 2013.

This paper is an extended version of [58], presented in *International Workshop on Telecommunications (IWT'2013)*, which was invited for publication in this journal.

A. A. Ferreira Júnior (antonioa@inatel.br / author for correspondence) and J. A. J. Ribeiro (justino@inatel.br) are with Instituto Nacional de Telecomunicações (INATEL), Santa Rita do Sapucaí, MG, Brazil.

O. L. Coutinho (olympio@ita.br) and J. E. B. Oliveira (edimar@ita.br) are with Instituto Tecnológico de Aeronáutica (ITA), São José dos Campos, SP, Brazil.

C. S. Martins (carla@ipqm.mar.mil.br) is with Instituto de Pesquisas da Marinha (IPqM), Rio de Janeiro, RJ, Brazil.

V. R. Almeida (vilson@ieav.cta.br) is with Instituto de Estudos Avançados (IEAv-DCTA), São José dos Campos, SP, Brazil.

The broadband and low loss offered by optical fiber communication led to interest in implementation and design of photonic assisted solutions for long-haul high-capacity communications systems. The majority of worldwide communications services as voice, data, video, and advanced internet applications are transported using optical fibers, forming an interconnected global optical network. The desire for high-capacity per fiber and low cost per information transmitted led to researches in optically networks with high spectral efficiencies. The demand for high-capacity and wide bandwidth increases at about 60% per year. Advanced optical modulation formats have become the key to the design of modern optical fiber communication systems [15]-[17].

Analog photonic links have attracted significant interest in many applications, such as phased-array antennas, radar systems, wireless communications RoF access, broadband cable-television networks, etc. [18]-[23]. Nowadays, the use of large value of modulation index became attractive in instrumentation and waveform generation applications. The high-frequency characterization and the measure of modulation efficiency of an optical modulator have been proposed [24]. A high resolution and wideband optical vector network analyzer was demonstrated with single and double sideband optical modulators [25]-[27]. A triangular pulse generator was proposed based on photonic-assisted devices [28].

A conventional external modulation process with a dual-drive integrated electrooptic Mach-Zehnder modulator (DD-MZM) based on intensity modulation and direct-detection techniques (IM-DD) was discussed by many authors. Assuming a balanced 50/50 splitting ratio of the DD-MZM's Y-junctions, an analysis of the chromatic dispersion effect on the performance of the analog link is given by [29] but the expressions there are in the form of infinite series. Such drawback is overcome in [30] where an analytical model in which the modulation indexes of the two DD-MZM drives can be unbalanced, yields a closed-form expressions for the power at the output of the detector. The electrooptical RF harmonic generation using an exact frequency domain analytical model of the link was discussed in [31]. This model is in agreement with theoretical and experimental results obtained in previously publications, which the expressions are in infinite series form and small-signal condition [32]-[33].

This paper deals with the fiber optic chromatic dispersion effect on the performance of an analog optical link based on IM-DD technique. The object is a RF up-conversion by using microwave photonic devices. An IM-DD link model which emphasizes both the external modulator electronic drive and the dispersion characteristic of a standard single-mode linear optical fiber (SSMF) is discussed. With DD-MZM at the nonlinear transmission bias points, minimum (MITB) and maximum (MATB), instead of quadrature bias point (QB), the effect of chromatic dispersion on the detected power may be mitigated with the optical bandwidth increasing. It is worthwhile to point out that the model enables large RF modulation index analysis, permits one to quickly retrieve a wide range of known results available on a rather ample literature regarding to this subject, and reduced numerical simulation time. Furthermore, an exact frequency domain analytical model approach which yields a rather insightful analysis of the link performance is presented. The model usefulness is illustrated by predicting the performance dependence on a direct-detection analog optical fiber link relating to link length, and is very helpful for system design. Some preliminary numerical simulations for a link which comprises optoelectronic components for practical application are given.

This publication consists of four other sections. The Section II gives an overview of the optical link components. An exact frequency domain analytical model for an analog optical fiber link is discussed in Section III. Numerical simulated results are presented and discussed in Section IV, and a few conclusions are presented in Section V.

II. Statement of the Problem

A simple block diagram of an optical fiber link is shown in Fig. 2, where different types of optical and optoelectronic components can be used to implement a modern optical fiber system [34]. The electrical signal is converted to optical signal (E/O conversion) by using direct or external modulation processes, and will be transported over the fiber link. At the receiver, a photodiode is used to convert the optical signal to electrical signal (O/E conversion). It should be pointed out that the optical intensity modulator and the square-law photodetector are nonlinear devices, in which introduce RF distortions into the system. Also, the effect of fiber chromatic dispersion will limit the transmission distance in a long-haul optical link, as well the optical signal may experience fiber nonlinearities, if the optical power is large to excite the nonlinear fiber effects. So, it is important to mitigate these impairments to improve the signal quality and system performance [35].

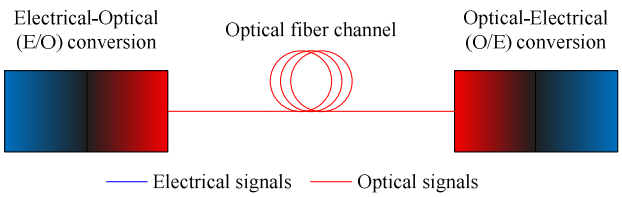

Fig. 2. A simple block diagram of an optical fiber link.

This paper is focused on a typical schematic representation of the IM-DD link to achieve a RF up-conversion, with a transmitter, an optical channel, and a receiver, as illustrated in Fig. 3(a). An intermediate frequency (IF) signal directs modulate a distributed feedback laser diode (DFB-LD) that feeds a DD-MZM imposing a local oscillator (LO) signal on optical carrier. The DD-MZM output signal is applied to an optical fiber link and at its output a square law photodetector (PD) is employed to recover the RF signal. This configuration

permits to modify the high-frequency and power requirements on the LO source [36]-[37]. The electronic driver of DD-MZM is emphasized in Fig. 3(b). A great deal of such control may be achieved through the drive electronics, by choosing the phase shift (θ_1) and the bias (θ_2) of the electrical signal applied to the modulator electrodes, as indicated in this figure.

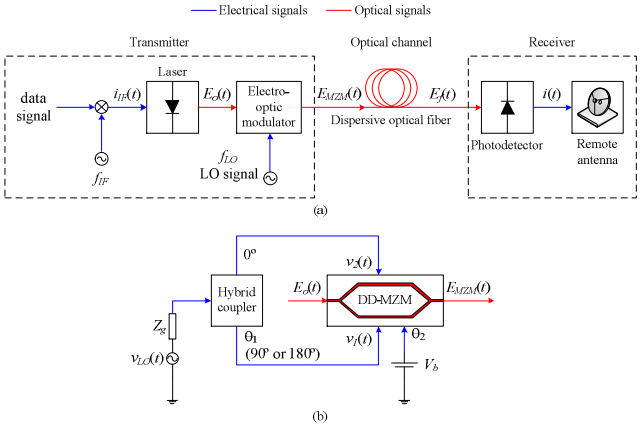

Fig. 3. (a) Overall architecture of fiber optic link with the transmitter, optical channel and receiver, and (b) the electronic driver of DD-MZM.

At the link input, a DFB-LD generates a carrier at a desired optical wavelength/frequency which is direct modulated by an IF signal. The output complex optical field is given by

$$E_o(t) = \sqrt{2\xi P_o(t)}\left[1 + m_i \cos(\omega_{IF} t)\right] e^{j[\omega_o t + \phi_o]} \qquad (1)$$

where ω_o is the mean optical frequency, ϕ_o is an arbitrary initial optical phase, $P_o(t)$ is the optical power, ξ (Ω/m^2) is a constant which depends on both the laser beam effective cross-section and the optical wave impedance, ω_{IF} is the angular frequency of IF signal, and m_i is the laser modulation index. This publication relies on the often used approach in the analysis of IM-DD optical links according to which the laser average power and its phase are time invariant. Fig 4 shows the DFB-LD output spectrum considering the small-signal condition and the first sidebands.

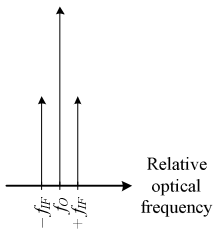

Fig. 4. DFB-LD output spectrum considering the small-signal condition and the first sidebands.

The simplified view of an integrated DD-MZM is illustrated in Fig. 5, where Fig. 5(a) shows the top view in which the optical waveguides are properly positioned with respect to the RF modulation field pattern, and Fig. 5(b) shows the cross-section view [38]-[39]. In Fig. 5(a) one should notice that the optical power delivered by the laser diode reaches the input Y-junction of the integrated z-cut $LiNbO_3$ DD-MZM and then is divided into two parcels according to a splitting ratio, determined by the Y-junction power transmission coefficient r_1 [40]. Once a MZM's configuration is specified, its performance dependence on substrate orientation and electrodes geometry can be predicted through the variation of the optical phase factor. Using a standard perturbation analysis such variation turns out to be [41]

$$\Delta\beta_{op}^{TE,TM} = \frac{\omega_o^2 \mu \varepsilon_0}{2\beta_{op}^{TE,TM}} \times \frac{\int_{-\infty}^{+\infty}\int_{-\infty}^{+\infty} \vec{E}^*_{TE,TM}(x,z) \cdot \left[-\varepsilon_{ii}\varepsilon_{jj} r_{ijk} E_k^{(m)}(x,z)\right] \vec{E}_{TE,TM}(x,z)\, dx dz}{\int_{-\infty}^{+\infty}\int_{-\infty}^{+\infty} \vec{E}^*_{TE,TM}(x,z) \bullet \vec{E}_{TE,TM}(x,z)\, dx dz} \qquad (2)$$

where $\beta_{op}^{TE,TM}$ and $E_{TE,TM}$ are the unperturbed optical phase factor and electric field for transverse electric (TE) or transverse magnetic (TM) modes, respectively, $E_k^{(m)}$ is the RF modulation electric field, r_{ijk} and ε_{ii} are the components of the electrooptic tensor and electric permittivity of $LiNbO_3$, respectively. Equation (2) shows that as consequence of the electrooptic effect a RF signal can be used to control the phase of the optical field associated with each optical power parcels as they propagates through the distinct arms of the DD-MZM. It is worthwhile to point out that in the configuration selected in Fig. 5 the optical guided mode has TM polarization, because it enables the utilization of the strongest $LiNbO_3$ electrooptic coefficient, namely r_{33}. The chosen substrate crystal cut orientation has the advantage of minimizes the fraction of chirping effect caused by the substrate properties [42]-[44]. The influence of this effect in the fiber length was observed in [45].

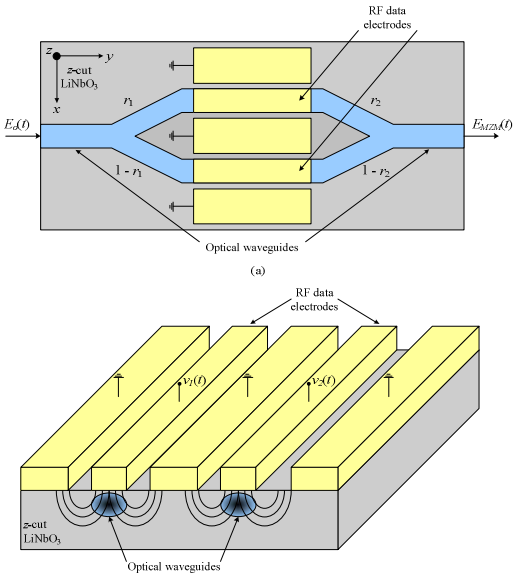

Fig. 5. Simplified integrated DD-MZM with a z-cut $LiNbO_3$ substrate using an optical TM mode, where (a) is the top view showing the Y-junctions transmission coefficients, and (b) shows the cross-section view.

The RF signal, henceforth named local oscillator (LO) signal according to Fig. 3, must generate an electric field having both a temporal and a spatial pattern adequately distribute in order to reach some key requirements performance, such as low RF power consumption and wide RF bandwidth [46]-[47]. It is worthwhile to point out that the DD-MZM plays an important role in the link for it enables the wideband implementation of single (OSSB) and double sideband (ODSB) analog optical modulation formats [48]-[49]. A LO signal driving the DD-MZM imposing a LO output signal on the optical carrier and a photonic up-conversion is achieved, i.e., the DD-MZM plays a role as a photonic mixer.

According to Fig. 3, the instantaneous values of the modulating signals applied to the lower and upper electrodes of MZM, are, respectively,

$$v_1(t) = V_1 \cos(\omega_{LO} t + \theta_1) \tag{3.a}$$

$$v_2(t) = V_2 \cos(\omega_{LO} t) \tag{3.b}$$

where V_1 and V_2 are the signals amplitudes in the lower and upper arms, ω_{LO} is the angular frequency of LO signal, and θ_1 is the phase difference between the signals. The optical phase variations introduced in the arms of the modulator through linear electrooptic effect are given by

$$\phi_1(t) = \frac{\pi}{V_\pi} v_1(t) = m_1 \cos(\omega_{LO} t + \theta_1) \tag{4.a}$$

$$\phi_2(t) = \frac{\pi}{V_\pi} v_2(t) = m_2 \cos(\omega_{LO} t) \tag{4.b}$$

$$\phi_b(t) = \frac{\pi}{V_\pi} V_b = \theta_2 \tag{4.c}$$

where V_π is the MZM half-wave switching voltage which can be calculated using (2), θ_2 is the phase variation due to the voltage bias applied to the proper access. The coefficients m_1 and m_2 are the modulation indexes due to the modulating signals in the lower and upper arms given, respectively, by

$$m_1 = \frac{\pi V_1}{V_\pi} \tag{5.a}$$

$$m_2 = \frac{\pi V_2}{V_\pi} \tag{5.b}$$

Based on the schematic representation illustrated in Fig. 5(a) and taking into account the splitting ratio of the output Y-junction r_2, it can be shown that the optical electrical field at the output of the DD-MZM has a complex form given by

$$E_{MZM}(t) = E_o e^{j\omega_o t}\left[1 + m_i \cos(\omega_{IF} t)\right] \times \times \left\{\sqrt{a}\, e^{j\left[m_1 \cos(\omega_{LO} t + \theta_1) + \theta_2\right]} + \sqrt{b}\, e^{j m_2 \cos(\omega_{LO} t)}\right\} \tag{6}$$

where $E_o = \sqrt{(2\xi P_o)}$, $a = r_1 r_2$, and $b = (1 - r_1)(1 - r_2)$. It should be pointed out that (6) applies to DD-MZM having both arbitrary splitting ratio and modulation signals. The fabrication tolerances make a balanced DD-MZM's particularly difficult to achieve, hence practical modulators have a finite extinction ratio. Such general situation often occurs in the real world, either at the modulator's fabrication stage or in field applications. This publication is concerned with links based on DD-MZM having a 50/50 splitting ratio. Hence, using (6), the output electrical field turns out to be expressed as

$$E_{MZM}(t) = \frac{E_o}{2} \sum_{n=-\infty}^{+\infty} a_n \left[e^{j(\omega_o + n\omega_{LO})t} + + \frac{m_i}{2} e^{j(\omega_o + n\omega_{LO} + \omega_{IF})t} + \frac{m_i}{2} e^{j(\omega_o + n\omega_{LO} - \omega_{IF})t} \right] \tag{7}$$

where

$$a_n = j^n \left[J_n(m_1) e^{j(n\theta_1 + \theta_2)} + J_n(m_2) \right] \tag{8}$$

and $J_n(.)$ is the first kind Bessel function with order n. It is readily seen that the optical field indeed consist of an infinite series of optical spectral components, i.e., an optical carrier component at ω_o and an infinite number of sidebands, with frequencies $\omega = \omega_o + n\omega_{LO}$ and $\omega = \omega_o + n\omega_{LO} \pm \omega_{IF}$, and amplitude a_n. A small-signal analysis in which enables one to identify the requirement which should be satisfied by the DD-MZM drive electronics in order to provide specific modulation formats was performed in [50]. For example, OSSB and ODSB modulation formats can be obtained when the pair of parameters (θ_1, θ_2) obeys the following constraints $(\pi/2, \pi/2)$ and $(\pi, \pi/2)$, respectively.

The output spectrums for the ODSB case with the DD-MZM at QB, MATB and MITB points are illustrated in Fig. 6. The LO harmonic order (n) varies from –4 to +4. In Fig. 6(a), all the sidebands are presented and refer to QB case. The MATB situation is illustrated in Fig. 6(b), where the odd spectral components are suppressed. The MITB case, Fig. 6(c), results in a suppressed carrier with suppressed even spectral components, as presented in Fig. 6(c).

The modulator output signal feeds a linear standard single-mode optical fiber (SSMF) with a step-index profile, circular dielectric waveguide and length L, as illustrated in Fig. 7. This simplified representation has n_1 and n_2 as the refractive indexes of the core and cladding with radius a and b, respectively [51]. As an example, a typical values of core and cladding diameters of a commercial SSMF is 8,2μm and 125μm, respectively [52].

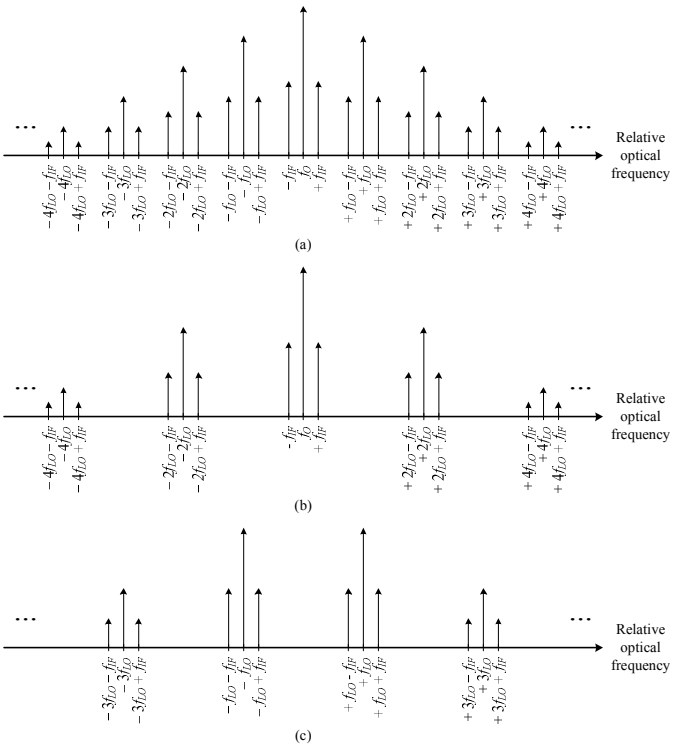

Fig. 6. The DD-MZM output spectrums for (a) QB (π,π/2), (b) MATB (π,0), and (c) MITB (π,π). The LO harmonic order (*n*) varies from –4 to +4.

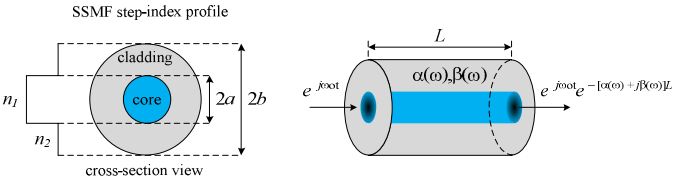

Fig. 7. Simplified representation of a step-index profile SSMF with circular dielectric waveguide with length *L*.

For instance, in the fiber modeling, a fused silica glass SSMF operating at 1550nm wavelength is considered with constant loss α(ω) (dB/km), whereas the phase factor β(ω) (rad/m) exhibits dependence with respect to the frequency deviation and chromatic dispersion. The optical signal is affected by the attenuation and the phase factors after propagates through a fiber with length *L*, as shown in Fig. 7. In the model of fiber optic propagation characteristics, one should bear in mind the presence of some phenomena in the fiber channel, which are different in nature, occur simultaneously, and influence each other, namely: noise, filtering, nonlinear effects, and polarization mode dispersion. These effects impose limitations on the performance in modern optical transmission systems [15],[53]. This publication is concerned with the filtering phenomenon which stems from the fiber's chromatic dispersion, including waveguide and material [16]. With respect to the SSMF attenuation, the 1550nm transmission window has the lowest attenuation value, around 0.2dB/km, compared with 1310nm transmission window, which is around 0.35dB/km [15]. However, the SSMF chromatic dispersion value at 1550nm is around 17ps/(nm.km), while at 1310nm has zero-dispersion [54].

In order to achieve a desired value for the chromatic dispersion parameter, some techniques to design optical fibers have been developed with index profiles often used to this purpose, as the nonzero-dispersion shifted (NZ-DSF) and the zero-dispersion shifted (DSF) [54]-[55]. The 1550nm window (C-band) is widely used for long-haul transmission system and the advance in research of erbium-doped fibers amplifiers made possible the use of this device in wavelength-division multiplexing systems. However, the DSF were not suitable for this system, because the nonlinear effect of four-wave mixing is the strongest when the dispersion is zero. Certain amount of dispersion is desirable to reduce this effect and the NZ-DSF was proposed.

All the optical signal spectral components will propagate through the optical fiber with different velocities and the phase of each component will be changed by chromatic dispersion. Bearing in mind that an exact functional form is rarely know, it is useful to expand it in Taylor series around the carrier frequency ω_o as [55]

$$\beta(\omega) = \beta_0(\omega_o) + \beta_1(\omega_o)(\omega-\omega_o) + \frac{1}{2}\beta_2(\omega_o)(\omega-\omega_o)^2 + \frac{1}{6}\beta_3(\omega_o)(\omega-\omega_o)^3 + \cdots \quad (9)$$

It is worthwhile to point out that the high order terms were not considered. The four terms on the right hand side shows distinct dependence with respect on the frequency deviation. The first term is constant and related to phase velocity of optical carrier, the second varies linearly and $\beta_1(\omega_o)$ determines the group velocity that is related to the group delay. The third one has a quadratic dependence and is related to the derivative of group velocity with respect to frequency. The $\beta_2(\omega_o)$ coefficient is related to the fiber chromatic dispersion parameter $D(\lambda)$, the optical carrier wavelength (λ_o), and the speed of light (*c*) in vacuum, according to following expression [55]

$$\beta_2(\omega_o) = -\frac{D(\lambda)\lambda_o^2}{2\pi c} \quad (10)$$

While the phase factor β(ω) exhibits dependence with respect to the frequency, the chromatic dispersion parameter $D(\lambda)$ has dependence with optical wavelength and can be modeled by a Taylor series expansion around the operation wavelength [56]. The $\beta_3(\omega_o)$ parameter in (9) can be obtained from the high order derivatives of phase factor, or is defined as the derivative of $\beta_2(\omega_o)$ with respect to frequency. It contributes to the calculation of the dispersion slope $S(\lambda)$, which has dependence with optical wavelength [16].

At the output end of the SSMF a square law PD transform the photon stream into a RF electric current. Introducing the concept of PD responsivity it can be shown that the electrical photocurrent is proportional to the incident average optical power, hence it is proportional to the magnitude of the optical

Poynting vector. Assuming a uniform power distribution over the fiber cross-section, the time dependent RF current is

$$i(t)=\Re\frac{E_f(t)E_f^*(t)}{2\xi}+n(t) \tag{11}$$

where $\Re$ is the PD responsivity, ξ (Ω/m^2) is a constant which depends on both the fiber effective cross-section and the optical wave impedance, and $E_f(t)$ is the optical electrical field at the fiber link output according to Fig. 3(a). The $n(t)$ term accounts for PD additive noises sources such as thermal and shot noises [14],[51], and this subject will not be addressed in this publication. By applying the fiber output to the PD, beating signals between the optical spectral components will generate harmonics of the original LO signal associated with IF signal. The characteristics of these signals depend on both the optical fiber chromatic dispersion and the modulation format. Such dependence will be used to estimate the link performance.

III. Optical fiber link model

In order to develop the analysis of the link, we consider a linear SSMF. Bearing in mind the spectral composition of the optical field at the output of the DD-MZM, we tackled the effect of the chromatic dispersion with the help of (9). The phase factor has optical spectral components with frequencies deviations equals to $\omega=\omega_o+n\omega_{LO}$ and $\omega=\omega_o+n\omega_{LO}\pm\omega_{IF}$. Therefore it might be possible to benefit from standard techniques developed for frequency domain analysis of a linear systems [30],[57]. Taking the Fourier transform of (7), we obtained the following expression for the output electrical field after propagates through a fiber with length L in the frequency domain [58]

$$\begin{aligned}E_f(\omega,L)=&\,2\pi\cdot10^{\frac{-\alpha_{dB}L}{20}}\frac{E_o}{2}\sum_{n=-\infty}^{+\infty}a_n\times\\&\times\left[\delta(\omega-\omega_o-n\omega_{LO})e^{j\frac{1}{2}n^2\omega_{LO}^2\beta_2(\omega_o)L}+\right.\\&+\frac{m_i}{2}\delta(\omega-\omega_o-n\omega_{LO}-\omega_{IF})e^{j\frac{1}{2}(n\omega_{LO}+\omega_{IF})^2\beta_2(\omega_o)L}+\\&\left.+\frac{m_i}{2}\delta(\omega-\omega_o-n\omega_{LO}+\omega_{IF})e^{j\frac{1}{2}(n\omega_{LO}-\omega_{IF})^2\beta_2(\omega_o)L}\right]\end{aligned} \tag{12}$$

where the δ symbol represents the Dirac delta function. To detect the RF current at output of the PD, we must be able to use the model to predict dependence on frequency of such current. To this aim, we first remember that the convolution theorem can be applied to rewrite the time domain expression of the PD current, given in (11), in the frequency domain as

$$I(\omega,L)=\Re\frac{E_f(\omega,L)*E_f^*(\omega,L)}{4\pi\xi} \tag{13}$$

where the mathematical symbol * denote convolution. We are interesting in just the terms that yield frequencies equals to $\omega_{RF}=k\omega_{LO}+\omega_{IF}$, and we obtain the following expression for the RF current Fourier's transform, under the condition $n=p+k$

$$I(\omega_{RF},L)=10^{\frac{-\alpha_{dB}L}{10}}\frac{\Re P_o m_i}{4}e^{j\frac{k\phi}{2}}\cos\left[\frac{\psi}{2}\right]\sum_{p=-\infty}^{+\infty}a_{p+k}a_p^*e^{jp\phi} \tag{14}$$

where

$$\phi=\omega_{LO}(k\omega_{LO}+\omega_{IF})\beta_2(\omega_o)L \tag{15}$$

$$\psi=\omega_{IF}(k\omega_{LO}+\omega_{IF})\beta_2(\omega_o)L \tag{16}$$

Until a few years ago, using such formulas to predict the spectral components of the PD current was rather cumbersome and yielded little physical insight, except when one assumed a small-signal approximation. It is worth to remember such complexity mostly stems from the fact that the coefficient $a_{p+k}a_p^*$ involves the product of Bessel's function, as it is readily seen in (8). However, such drawback was overcome through the application of addition theorem for Bessel functions [30],[59]. In order to be able to take advantage of such theorem in the analysis presented in this publication, we first use (8) to calculate $a_{p+k}a_p^*$, and after some mathematical manipulations we obtained an expression for $I(\omega_{RF},L)$. The result allows one to retrieve previous publications and also includes a few practical parameters such as the fiber attenuation and chromatic dispersion, PD responsivity, and the output power and modulation index of the laser. Such expression is given by

$$\begin{aligned}I(\omega_{RF},L)=&\,10^{\frac{-\alpha_{dB}L}{10}}\frac{\Re P_o m_i}{4}\cos\left[\frac{\psi}{2}\right]\times\\&\times\left\{e^{jk\left(\theta_1+\frac{\phi+\pi}{2}\right)}\sum_{p=-\infty}^{+\infty}J_{p+k}(m_1)J_p(m_1)e^{jp\phi}+\right.\\&+e^{jk\left(\frac{\phi+\pi}{2}\right)}\sum_{p=-\infty}^{+\infty}J_{p+k}(m_2)J_p(m_2)e^{jp\phi}+\\&+e^{j\left[k\left(\theta_1+\frac{\phi+\pi}{2}\right)+\theta_2\right]}\sum_{p=-\infty}^{+\infty}J_{p+k}(m_1)J_p(m_2)e^{jp(\phi+\theta_1)}+\\&\left.+e^{j\left[N\left(\frac{\phi+\pi}{2}\right)-\theta_2\right]}\sum_{p=-\infty}^{+\infty}J_{p+k}(m_2)J_p(m_1)e^{jp(\phi-\theta_1)}\right\}\end{aligned} \tag{17}$$

It is worth noting that (17) were obtained without introducing any approximation. Furthermore, (6) and (17) enables one quickly retrieve the results for DD-MZM having infinite extinction ratio ($r_1=r_2=0.5$) and when the modulation indexes are equal ($m_1=m_2=m$). Since we intend to compare our predictions with previous publication, we apply the addition

theorem for Bessel functions [60] to (17) under the assumption that the modulation indexes are equal and with $\theta_1=\pi$ (ODSB case). We obtain

$$I(\omega_{RF},L)= 10^{\frac{-\alpha_{dB}L}{10}}\frac{(-1)^k\Re P_o m_i}{4}\cos\left[\frac{\psi}{2}\right]\times \times\left\{\left[1+(-1)^k\right]J_k\left[2m\sin\left(\frac{\phi}{2}\right)\right]+ +(j)^k\left\{e^{j\theta_2}J_k\left[2m\sin\left(\frac{\phi+\pi}{2}\right)\right]+ +e^{-j\theta_2}J_k\left[2m\sin\left(\frac{\phi-\pi}{2}\right)\right]\right\}\right\} \quad (18)$$

In this publication, the modeling of the analog optical fiber link is synthesized by (18). It enables the frequency domain analysis of how the optical fiber chromatic dispersion affects the link performance which employs direct modulation of laser and external modulation to achieve RF up-conversion. The ϕ parameter, which is given in (15), taking into account the LO harmonic order, LO frequency and IF, chromatic dispersion and optical fiber length. The link performance can be evaluated in terms of the RF output average power delivered to load (R_L) as

$$P_{R_L}(\omega_{RF},L)=\frac{1}{2}\left|I(\omega_{RF},L)\right|^2 Z_L \quad (19)$$

Impedances matching networks are often used at the DD-MZM input and PD output to provide the maximum signal power transfer, due to the frequency response of these devices. In this work, all the impedances were considered purely resistive and matched. The modulation index (m) is related to signal power (P_{RF}) and impedance (Z_g) of the RF source, and to the DD-MZM input impedance (Z_{MZM}). The RF power delivered to the load (P_{RL}) is related to the PD output impedance [61]. By using (18), it is possible to define the normalized power penalty (PP) parameter, caused by the dispersion-induced effect, as the ratio between the power loss in detected electrical signals with and without the effect of chromatic dispersion parameter [36]-[37]. We obtain the following exact frequency domain expression which also enables the analysis with any modulation index value (m)

$$PP=\frac{\left|\cos\left(\frac{\psi}{2}\right)\left\{\begin{array}{l}\left[1+(-1)^k\right]J_k\left[2m\sin\left(\frac{\phi}{2}\right)\right]+\\ +j^k\left\{\begin{array}{l}e^{j\theta_2}J_k\left[2m\sin\left(\frac{\phi+\pi}{2}\right)\right]+\\ +e^{-j\theta_2}J_k\left[2m\sin\left(\frac{\phi-\pi}{2}\right)\right]\end{array}\right.\end{array}\right\}\right|^2}{\left|\left[1+(-1)^k\right]J_k(0)+j^kJ_k(2m)\left[e^{j\theta_2}+(-1)^k e^{-j\theta_2}\right]\right|^2} \quad (20)$$

IV. Numerical Results

The numerical simulations were developed by using parameters specified in Table I. To validate our model, first of all we developed simulation allowing the recovering previous results and modeling [36]-[37]. Some detected electrical power results are presented in Fig. 8 and Fig. 9, under specified conditions. The RF and IF are 30GHz and 1GHz, respectively, and the signals phase shift (θ_1) applied to DD-MZM electrodes is π. In both figures the conventional ODSB case is obtained when $\theta_2=\pi/2$.

TABLE I
Typical values of parameters used in the simulation.

Parameter description	Symbol	Value
RF source impedance	Z_g	50Ω
RF load impedance	Z_L	50Ω
Power applied to the DD-MZM	P_{RF}	10mW
Laser output optical power	P_o	1mW
Laser wavelength	λ_o	1550nm
Laser modulation index	m_i	0.5
DD-MZM half-wave voltage	V_π	5V
DD-MZM input impedance	Z_{MZM}	50Ω
Fiber attenuation [52]	α_{dB}	0.2dB/km
Fiber chromatic dispersion [52]	D	17ps/(nm.km)
Speed of light in vacuum	c	$3x10^8$m/s
PD responsivity [62]	$\Re$	0.75A/W

In Fig. 8, it was used the LO second harmonic (k=2) with 14.5GHz frequency. It is observed that by biasing the DD-MZM at minimum transmission bias point (MITB), i.e. $\theta_2=\pi$, the effect of optic fiber chromatic dispersion is mitigated if compared to the other bias points. This behavior is the same for the LO harmonic orders that obeys the relation given by $2+4N$, with N=0, 1, 2, ….

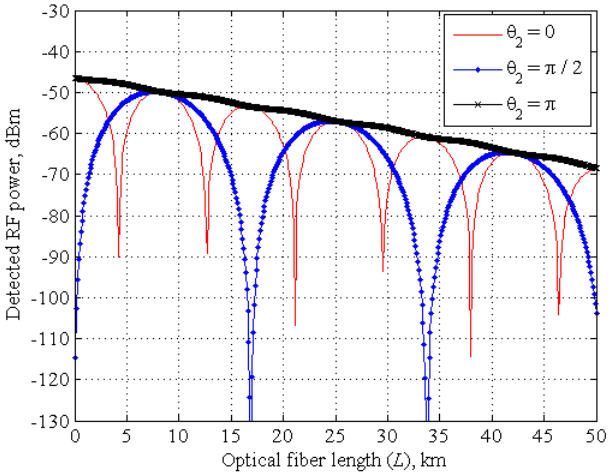

Fig. 8. Detected RF power versus fiber optic length, using LO second harmonic (k=2), with $\theta_1=\pi$ and θ_2 as a parameter. The RF, IF and LO frequency are 30GHz, 1GHz and 14.5GHz, respectively.

In Fig. 9, the LO fourth harmonic (k=4) was used and its frequency is reduced to 7.25GHz. In this case, the chromatic dispersion effect is less sensitive when the DD-MZM is biased

at maximum transmission bias point (MATB) condition, i.e. θ_2=0, if compared to the other bias points. In this case, the results are the same for LO harmonic orders equals to 4+4*N*, with *N*=0, 1, 2, …. In this situation, the power of the received signal is reduced, as expected, because the use of high LO harmonic order. However, the DD-MZM was biased with less energy if compared with MITB case.

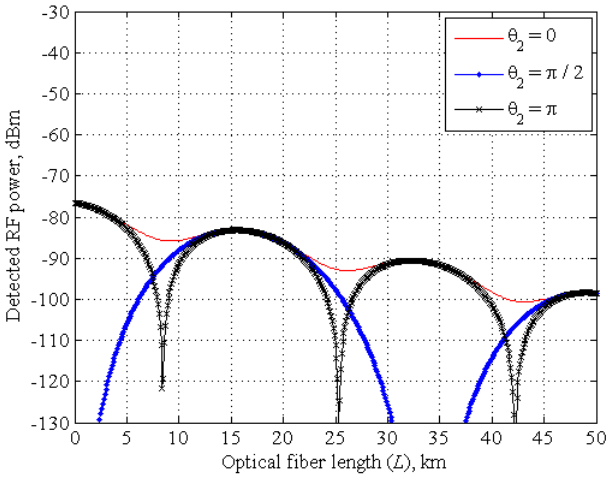

Fig. 9. Detected RF power versus fiber optic length, using LO fourth harmonic (*k*=4), with θ_1=π and θ_2 as a parameter. The RF, IF and LO frequency are 30GHz, 1GHz and 7.25GHz, respectively.

The power penalty (*PP*) in function of optical fiber length (*L*) with f_{IF} as a parameter and RF equal to 30GHz was evaluated. In Fig. 10, the LO second harmonic (*k*=2) was used and correspond to MITB (θ_2=π) situation. In Fig. 11, MATB (θ_2=0) case, the LO fourth harmonic (*k*=4) was considered. In both figures, it is observed that the intermediate frequency (IF) limits the link response, as its value increase.

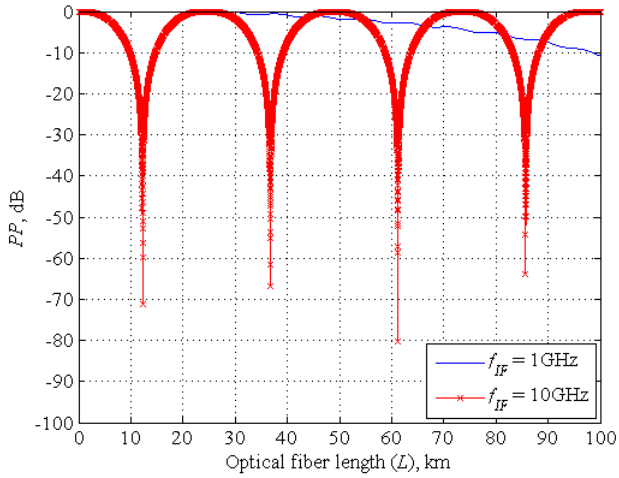

Fig. 10. Power penalty (*PP*) versus optical fiber length (*L*) for the MITB case (θ_2=π) with *k*=2. The RF frequency is 30GHz with f_{IF} as a parameter.

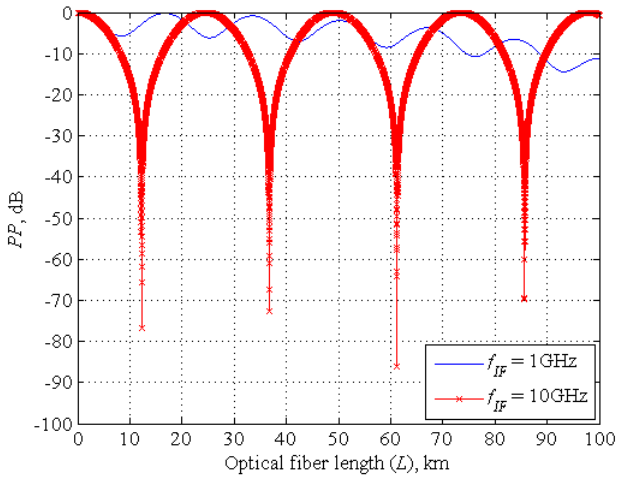

Fig. 11. Power penalty (*PP*) versus optical fiber length (*L*) for the MATB case (θ_2=0) with *k*=4. The RF frequency is 30GHz with f_{IF} as a parameter.

V. Final Comments

This publication presented a very comprehensive exact frequency domain analytical model, which enables the analysis of the optical fiber chromatic dispersion effect on the performance of an analog fiber link with direct modulation of laser and by using a DD-MZM to achieve a RF up-conversion. It is observed that it is possible reduce the LO source high-frequency to generate a desired RF frequency by using microwave photonic devices.

The model besides relaying on parameters which are suited to experimental researchers, also allows one to retrieve important results available in a very wide literature. Using some components and devices we performed numerical simulations which yielded results which seem to be of practical interest. The authors are working towards designing, implementing and characterizing fiber link based on the model developed.

Acknowledgments

To the Electronic Warfare Laboratory at the Instituto Tecnológico de Aeronáutica (ITA) and the Instituto Nacional de Telecomunicações (INATEL) for their support in this research.

References

[1] J. Capmany, J. Mora, I. Gasulla, J. Sancho, J. Lloret, S. Sales, "Microwave Photonic Signal Processing," *Journal of Lightwave Technolgy*, vol. 31, no. 4, pp. 571-586, February 2013.

[2] J. Yao, "A tutorial on microwave photonics I," *IEEE Photonics Society Newsletter*, vol. 26, no. 2, pp. 4-12, April 2012.

[3] J. Yao, "A tutorial on microwave photonics II," *IEEE Photonics Society Newsletter*, vol. 26, no. 3, pp. 5-12, June 2012.

[4] A. J. Seeds, K. J. Williams, "Microwave Photonics," *Journal of Lightwave Technolgy*, vol. 24, no. 12, pp. 4628-4641, December 2006.

[5] A. J. Seeds, C.-P. Liu, T. Ismail, M. J. Fice, F. Pozzi, R. J. Steed, E. Rouvalis, C. C. Renaud, "Microwave Photonics," in *Conference on Lasers and Electro-Optics (CLEO) and Quantum Electronics and Laser Science Conference (QELS)*, pp. 1-2, May 2010.

[6] J. Capmany, B. Ortega, D. Pastor, "A Tutorial on Microwave Photonic Filters," *Journal of Lightwave Technology*, vol. 24, no. 1, pp. 201-229, January 2006.

[7] J. Martí, J. Capmany, "Microwave Photonics and Radio-over-Fiber Research," *IEEE Microwave Magazine*, vol. 10, no. 4, pp. 96-105, June 2009.

[8] V. J. Urick, F. Bucholtz, J. D. McKinney, P. S. Devgan, A. L. Campillo, J. L. Dexter, K. J. Williams, "Long-Haul Analog Photonics," *Journal of Lightwave Technology*, vol. 29, no. 8, pp. 1182-1205, April 2011.

[9] C. Lim, A. Nirmalathas, M. Bakaul, P. Gamage, K.-L. Lee, Y. Yang, D. Novak, R. Waterhouse, "Fiber-Wireless Networks and Subsystem Technologies," *Journal of Lightwave Technology*, vol. 28, no. 4, pp. 390-405, February 2010.

[10] J. Yao, "Microwave Photonics," in *IEEE International Workshop on Electromagnetics, Applications and Student Innovation (iWEM)*, pp. 1-2, August 2012.

[11] J. E. B. Oliveira, F. D. P. Alves, A. L. P. Mattei, "Trends in Photonics Applied to Electronic Warfare at Brazilian Airforce," in *International Microwave and Optoelectronics Conference (SBMO/IEEE MTT-S, APS and LEOS – IMOC'99)*, vol. 2, pp. 599-602, August 1999.

[12] O. L. Coutinho, V. R. Almeida, J. E. B. Oliveira, "Uso de Redes de Comunicações Ópticas para Transmissão e Distribuição de Emissores Radar," in *Simpósio de Aplicações Operacionais em Áreas de Defesa (XIII SIGE)*, pp. 1-8, Setembro 2011.

[13] O. L. Coutinho, V. R. Almeida, C. S. Martins, J. E. B. Oliveira, "Aplicação de Enlace a Fibra Óptica em Transmissão de Sinais de Radar," in *Simpósio Brasileiro de Microondas e Optoeletrônica (MOMAG)*, pp. 1-5, Setembro 2008.

[14] W. Lim, T.-S. Cho, K. Kim, C. Yun, "Analytical time-domain model for radio over free space optical military communication systems under turbulence channels," in *IEEE Military Communications Conference (MILCOM 2009)*, pp. 1-5, October 2009.

[15] R.-J. Essiambre, G. Kramer, P. J. Winzer, G. J. Foschini, B. Goebel, "Capacity Limits of Optical Fiber Networks," *Journal of Lightwave Technology*, vol. 28, no. 4, pp. 662-701, February 2010.

[16] P. J. Winzer, R.-J. Essiambre, "Advanced Optical Modulation Formats," *Proceedings of the IEEE*, vol. 94, no. 5, pp. 952-985, May 2006.

[17] P. J. Winzer, "Modulation and multiplexing in optical communication system," *IEEE LEOS News*, vol. 23, no. 1, pp. 4-10, February 2009.

[18] H. Zhang, S. Pan, M. Huang, X. Chen, "Polarization-modulated analog photonic link with compensation of the dispersion-induced power fading," *Optics Letters*, vol. 37, no. 5, pp. 866-868, March 2012.

[19] S. Li, X. Zheng, H. Zhang, B. Zhou, "Compensation of dispersion-induced power fading for highly linear radio-over-fiber link using carrier phase-shifted double sideband modulation," *Optics Letters*, vol. 36, no. 4, pp. 546-548, February 2011.

[20] G. Zhang, X. Zheng, S. Li, H. Zhang, B. Zhou, "Postcompensation for nonlinearity of Mach–Zehnder modulator in radio-over-fiber system based on second-order optical sideband processing," *Optics Letters*, vol. 37, no. 5, pp. 806-808, March 2012.

[21] B. Vidal, "Analytical model for hybrid amplitude and phase modulation in dispersive radio over fiber links," *Optics Communications*, vol. 284, no. 21, pp. 5138-5143, October 2011.

[22] B. Hraimel, X. Zhang, Y. Pei, K. Wu, T. Liu, T. Xu, Q. Nie, "Optical Single-Sideband Modulation With Tunable Optical Carrier to Sideband Ratio in Radio Over Fiber Systems," *Journal of Lightwave Technology*, vol. 29, no. 5, pp. 775-781, March 2011.

[23] P.-Y. Wu, H.-H. Lu, C.-L. Ying, C.-Y. Li, H.-S. Su, "An Upconverted Phase-Modulated Fiber Optical CATV Transport System," *Journal of Lightwave Technology*, vol. 29, no. 16, pp. 2422-2427, August 2011.

[24] S. Zhang, R. Lu, D. Chen, S. Liu, Y. Liu, "High-frequency characterization of an optical phase modulator with phase modulation-to-intensity modulation conversion in dispersive fiber," *Chinese Science Bulletin*, vol. 57, no. 22, pp. 2929-2933, August 2012.

[25] Z. Tang, S. Pan, J. Yao, "A high resolution optical vector network analyzer based on a wideband and wavelength-tunable optical single-sideband modulator," *Optics Express*, vol. 20, no. 6, pp. 6555-6560, March 2012.

[26] M. Xue, Y. Zhao, X. Gu, S. Pan, "Performance analysis of optical vector networks analyzer based on optical single-sideband modulation," *Journal of Optical Society of America B*, vol. 30, no. 4, pp. 928-933, April 2013.

[27] M. Wang, J. Yao, "Optical vector network analyzer based on unbalanced double-sideband modulation," *IEEE Photonics Technology Letters*, vol. 25, no. 8, pp. 753-756, April 2013.

[28] J. Li, X. Zhang, B. Hraimel, T. Ning, L. Pei, K. Wu, "Performance analysis of photonic-assisted periodic triangular-shaped pulses generator," *Journal of Lightwave Technology*, vol. 30, no. 11, pp. 1617-1624, June 2012.

[29] J. L. Corral, J. Marti, J. M. Fuster, "General expressions for IM/DD dispersive analog optical links with external modulation or optical up-conversion in Mach–Zehnder electrooptical modulator," *IEEE Transactions on Microwave Theory and Techniques*, vol. 49, no. 10, pp. 1968–1976, October 2001.

[30] L. Cheng, S. Aditya, A. Nirmalathas, "An Exact Analytical Model for Dispersive Transmission in Microwave Fiber-Optic Links Using Mach-Zehnder External Modulator," *IEEE Photonics Technology Letters*, vol. 17, no. 7, pp. 1525-1527, July 2005.

[31] A. A. Ferreira Jr., O. L. Coutinho, C. S. Martins, W. S. Fegadolli, J. A. J. Ribeiro, V. R. Almeida, J. E. B. Oliveira, "Effect of Fiber Optic Chromatic Dispersion on the Performance of Analog Optical Link with External Modulation Aiming at Aerospace Applications," *Journal of Aerospace Technology and Management*, vol. 5, no. 2, pp. 205-216, April-June 2013.

[32] J. Han, B.-J. Seo, Y. Han, B. Jalali, H. R. Fetterman, "Reduction of fiber chromatic dispersion effects in fiber-wireless and photonic time-stretching system using polymer modulators," *Journal of Lightwave Technology*, vol. 21, no. 6, pp. 1504-1509, June 2003.

[33] U. Gliese, S. Norskov, T. N. Nielsen, "Chromatic dispersion in fiber-optic microwave and millimeter-wave links," *IEEE Transactions on Microwave Theory and Techniques*, vol. 44, no. 10, pp. 1716-1724, October 1996.

[34] S. Iezekiel, "Measurements of Microwave Behavior in Optical Links," *IEEE Microwave Magazine*, vol. 9, no. 3, pp. 100-120, June 2008.

[35] C. Lim, A. Nirmalathas, M. Bakaul, K.-L. Lee, D. Novak, R. Waterhouse, "Mitigation strategy for transmission impairments in millimeter-wave radio-over-fiber networks," *Journal of Optical Networking*, vol. 8, no. 2, pp. 201-214, February 2009.

[36] J. M. Fuster, J. Marti, J. L. Corral, V. Polo, F. Ramos, "Generalized Study of Dispersion-Induced Power Penalty Mitigation Techniques in Milimeter-Wave Fiber-Optics Links," *Journal of Lightwave Technology*, vol. 18, no. 7, pp. 933-940, July 2000.

[37] B. Hraimel, R. Kashyap, J. X. Zhang, J. Yao, K. Wu, "Large Signal Analysis of Fiber Dispersion Effect on Photonic Up-Conversion in Radio over Fiber link using Dual Electrode Mach-Zehnder External Modulator," *Proceedings of SPIE 6343*, pp. 63432L-63432L-12, September 2006.

[38] M. Morant, R. Llorente, J. Hauden, T. Quinlan, A. Mottet, S. Walker, "Dual-drive $LiNbO_3$ interferometric Mach-Zehnder architecture with extended linear regime for high peak-to-average OFDM-based communication systems," *Optics Express*, vol. 19, no. 26, pp. B450-B456, December 2011.

[39] D. Janner, D. Tulli, M. Belmonte, V. Pruneri, "Waveguide electro-optic modulation in micro-engineered $LiNbO_3$," *Journal of Optics A: Pure and Applied Optics*, no. 10, pp. 1-6, 2008.

[40] C.-T. Lin, J. Chen, S.-P. Dai, P.-C. Peng, S. Chi, "Impact of Nonlinear Transfer Function and Imperfect Splitting Ratio of MZM on Optical Up-Conversion Employing Double Sideband With Carrier Suppression Modulation," *Journal of Lightwave Technology*, vol. 26, no. 15, pp. 2449-2459, August 2008.

[41] C. Kitano, J. E. B. Oliveira, "Projeto de Moduladores Eletroópticos Faixa Larga Utilizando Tecnologia de Óptica Integrada," *Revista Telecomunicações*, vol. 2, no. 2, pp. 5-16, setembro 1999.

[42] Y. Shi, L. Yan, A. E. Willner, "High-Speed Electrooptic Modulator Characterization Using Optical Spectrum Analysis," *Journal of Lightwave Technology*, vol. 21, no. 10, pp. 2358-2367, October 2003.

[43] X. Chen, S. Feng, D. Huang, "Impact of Mach-Zehnder Modulator Chirp on Radio over Fiber Links," *Journal of Infrared, Millimeter and Terahertz Waves*, vol. 30, no. 7, pp. 770–779, July 2009.

[44] C. E. Rogers III, J. L. Carini, J. A. Pechkis, P. L. Gould, "Characterization and compensation of the residual chirp in a Mach-Zehnder-type electro-optical intensity modulator," *Optics Express*, vol. 18, no. 2, pp. 1166-1176, January 2010.

[45] G. H. Smith, D. Novak, Z. Ahmed, "Overcoming Chromatic-Dispersion Effects in Fiber-Wireless Systems Incorporating External Modulators," *IEEE Transactions on Microwave Theory and Techniques*, vol. 45, no. 8, pp. 1410-1415, August 1997.

[46] C. Kitano, J. E. B. Oliveira, "Dispositivos à Óptica Integrada para Aplicações em Telecomunicações," *Revista Telecomunicações*, vol. 3, no. 2, pp. 27-38, Dezembro 2000.

[47] J. E. B. Oliveira, J. A. J. Ribeiro, "Interfaces para Enlaces de Fibra Óptica de Alta Velocidade," *Revista Telecomunicações*, vol. 3, no. 2, pp. 65-75, Dezembro 2000.

[48] W. S. Fegadolli, J. E. B. Oliveira, V. R. Almeida, "Highly linear electro-optic modulator based on ring resonator," *Microwave and Optical Technology Letters*, vol. 53, no. 10, pp. 2375-2378, October 2011.

[49] G. H. Smith, D. Novak, Z. Ahmed, "Technique for optical SSB generation to overcome dispersion penalties in fibre-radio systems," *Electronics Letters*, vol. 33, no. 1, pp. 74-75, January 1997.

[50] A. A. Ferreira Júnior, O. L. Coutinho, C. S. Martins, W. S. Fegadolli, J. A. J. Ribeiro, J. E. B. Oliveira, "Effect of Fiber Optic Chromatic Dispersion on the Performance of Analog Optical Link with Dual-Drive Mach-Zehnder Modulator," in *Simpósio de Aplicações Operacionais em Área de Defesa (XIV SIGE)*, pp. 119-126, Setembro 2012.

[51] A. Yariv, P. Yeh, P, "Photonics: Optical Electronics in Modern Communications," 6th edition, Oxford University Press: New York, 2007.

[52] Corning® SMF-28® Optical Fiber Product Information. From: http://www.corning.com/WorkArea/showcontent.aspx?id=41261. Access: June 25, 2013.

[53] L. G.-Nielsen, M. Wandel, P. Kristensen, C. Jorgensen, L. V. Jorgensen, B. Edvold, B. Pálsdóttir, D. Jakobsen, "Dispersion-Compensating Fibers," *Journal of Lightwave Technology*, vol. 23, no. 11, pp. 3566-3579, November 2005.

[54] M.-J. Li, D. A. Nolan, "Optical Transmission Fiber Design Evolution," *Journal of Lightwave Technology*, vol. 26, no. 9, pp. 1079-1092, May 2008.

[55] G. P. Agrawal, "Fiber-Optic Communication Systems," 3rd edition, John Wiley & Sons: New York, 2002.

[56] M. Wandel, P. Kristensen, "Fiber designs for high figure of merit and high slope dispersion compensating fibers," *Journal of Optical and Fiber Communications Research*, vol. 3, no. 1, pp. 25-60, February 2006.

[57] E. Vos, "Frequency Domain Approach for Optimizing Optical Frequency Multiplication System using Mach-Zehnder- and Fabry-Perot- Interferometer," in *Graduation Symposium – Eindhoven University of Technology*, pp. 1-12, August 2008.

[58] A. A. Ferreira Júnior, O. L. Coutinho, C. S. Martins, J. A. J. Ribeiro, V. R. Almeida, J. E. B. Oliveira, "Analytical model of optical fiber chromatic dispersion effect in up-converted millimeter-wave long-haul fiber optic link," in *International Workshop on Telecommunications (IWT)*, pp. 1-8, May 2013.

[59] H. Chi, J. Yao, "Power Distribution of Phase-Modulated Microwave Signals in a Dispersive Fiber-Optic Link," *IEEE Photonics Technology Letters*, vol. 20, no. 4, pp. 315-317, February 2008.

[60] M. Abramowitz, I. Stegun, "Handbook of Mathematical Functions with Formulas, Graphs, and Mathematical Tables," Dover Publications: New York, 1965.

[61] O. L. Coutinho, V. R. Almeida, J. E. B. Oliveira, "Analysis of analog fiber optical links based on DSB+C and SSB+C modulation techniques," in *International Conference on Microwave and Optoelectronics (SBMO/IEEE MTT-S)*, pp. 439-443, July 2005.

[62] ThorLabs DET10D. From: http://www.thorlabs.com/Thorcat/13100/DET10D-Manual.pdf. Access: June 25, 2013.

Antonio Alves Ferreira Júnior received the bachelor's degree in Electrical Engineering (2002) and the master's degree (2006) in Telecommunications Engineering, from Instituto Nacional de Telecomunicações (INATEL), Santa Rita do Sapucaí, Brazil. He is currently working toward to the doctorate in Electronic and Computer Engineering, with research focus on microwave photonics, at Instituto Tecnológico de Aeronáutica (ITA), São José dos Campos, Brazil. At INATEL, he is undergraduate professor, and he also worked with radio-frequency circuit designs. His interests include radio-frequency circuits, and microwave photonics.

Olympio Lucchini Coutinho was born in Belo Horizonte, Brazil, in 1966. He received the Degree of Electrical Engineer from Pontifícia Universidade Católica de Minas Gerais (1992). He received the M.Sc. Degree (2005) and the Ph.D. Degree (2011) in Electronic and Computer Engineering from Technological Institute of Aeronautics (ITA), in microwave and optoelectronic area. His is a Brazilian Air Force Officer, here he has been working with telecommunication, radio navigation, radar and electronic warfare. He is currently with ITA, where he has been teaching and leading the Electronic Warfare Laboratory. He has been working on microwave photonics and radar signal generation and analysis. His research area is fiber optic radar signal transmission, generation and processing.

Carla de Sousa Martins received her B.S. degree from Rio de Janeiro State University (UERJ) in 1996 and M.Sc degree from Aeronautics Institute of Technology (ITA) in 2009. She is currently the Coordinator of the Electronic Warfare Systems Research Group at Brazilian Navy Research Institute (IPqM). Her research mainly focuses on the development of advanced technologies applied to electronic warfare systems for surface, submarine and aerospace platforms. Her interest focuses on microwave photonics, which includes photonic processing of microwave signals, photonic generation of microwave and radio over fiber.

José Antônio Justino Ribeiro was born in Mimoso do Sul – State of Espírito Santo at August 02, 1946. He is an Electrical and Telecommunications Engineer through National Institute of Telecommunications (INATEL) and he holds a Master and Doctor of Science degrees, both in Electronic and Computer Engineering, through Technological Institute of Aeronautics, São José dos Campos, SP. He is a full professor at INATEL, at Federal University of Itajubá and at Francisco Moreira da Costa Electronics Technical Scholl. During more than 40 years he has taught various subjects in electronic and telecommunications fields in undergraduate and graduate courses. He has published several technical and scientific papers as author or co-author and he is author of four books in Portuguese by Erica Editions: *Optical Communications*, *Electromagnetic Waves Propagation*, *Microwave Engineering* and *Antenna Engineering*. He is a founding member of Brazilian Microwaves and Optoelectronic Society (SBMO) and a member of Brazilian Automatic Society (SBA), of Brazilian Engineering Teaching Association (ABENGE), of The Institute of Electrical and Electronic Engineers (IEEE) and of The International Society for Optical Engineering (SPIE).

Vilson Rosa de Almeida received his B.S. (Magna Cum Laude) and M.S., both in Electronics Engineering, from Instituto Tecnológico de Aeronáutica (ITA), Sao Jose dos Campos, Brazil, in 1997 and 1998, respectively. He received his Ph.D. degree from Cornell University in 2005, from the Dept. of Electrical and Computer Engineering, with research focus on Silicon Nanophotonics. Since 1998, he has worked as a photonics researcher at Instituto de Estudos Avançados (IEAv-CTA), Sao Jose dos Campos, Brazil, where currently holds the position of Director. He has also worked as a Graduate Professor at ITA since 2006. His research interest areas are silicon photonics, nanophotonic devices, and optical fiber sensors.

José Edimar Barbosa Oliveira received the B.S. degree in 1976 from Universidade de Brasília, Brasília, Brazil, the M.S. degree in 1979 from the Instituto Tecnológico de Aeronáutica (ITA), São José dos Campos, Brazil, and the Ph.D. degree in 1986 from the Electrical Engineering Department of McGill University, Montreal, Canada. Since 1977 he is with the Electronics Engineering Department at ITA, where he currently holds the position of full professor. His research interest areas are photonic and optoelectronic devices, and optical communications.